

See discussions, stats, and author profiles for this publication at: <https://www.researchgate.net/publication/273510915>

Self-Assembled 3D Graphene Monolith from Solution

ARTICLE *in* JOURNAL OF PHYSICAL CHEMISTRY LETTERS · FEBRUARY 2015

Impact Factor: 7.46 · DOI: 10.1021/jz502655m

CITATIONS

12

READS

236

4 AUTHORS, INCLUDING:



Wei Lv

Tsinghua University

72 PUBLICATIONS 2,018 CITATIONS

[SEE PROFILE](#)



Chun Yuan

Tsinghua University

160 PUBLICATIONS 2,802 CITATIONS

[SEE PROFILE](#)

Self-Assembled 3D Graphene Monolith from Solution

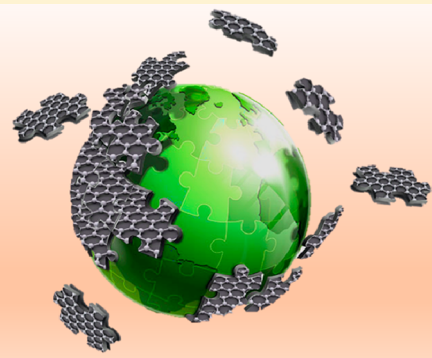
Wei Lv,[†] Chen Zhang,^{‡,§} Zhengjie Li,^{‡,§} and Quan-Hong Yang^{*,†,‡,§}

[†]Shenzhen Key Laboratory for Graphene-based Materials, Graduate School at Shenzhen, Tsinghua University, Shenzhen 518055, China

[‡]Key Laboratory for Green Chemical Technology of Ministry of Education, School of Chemical Engineering and Technology, Tianjin University, Tianjin 300072, China

[§]Collaborative Innovation Center of Chemical Science and Engineering (Tianjin), Tianjin 300072, China

ABSTRACT: Three-dimensional (3D) graphene-assembled monoliths (GAs), especially ones prepared by self-assembly in the liquid phase, represent promising forms to realize the practical applications of graphene due to their high surface utilization and operability. However, the understanding of the assembly process and structure control of 3D GAs, as a new class of carbon materials, is quite inadequate. In this Perspective, we give a demonstration of the assembly process and discuss the key factors involved in the structure control of 3D GAs to pave the way for their future applications. It is shown that the assembly process starts with the phase separation, which is responsible for the formation of the 3D networked structure and liquid phase as the spacers avoid the parallel overlap of graphene layers and help form an interlinked pore system. Well-tailored graphene sheets and selected assembly media must be a precondition for a well-controlled assembly process and microstructure of a 3D GA. The potential applications in energy storage featuring high rate and high volumetric energy density demonstrate advantages of 3D GAs in real applications.



Graphene refers to a monolayer of carbon atoms in a covalently bonded honeycomb arrangement that has been the subject of much research in recent years. It has many unique and excellent electronic, physical, and chemical properties and, thus, great potential in applications of superfast transistors, chemical and biosensors, energy storage, and conversion systems.^{1,2} However, random aggregation and overlaying of graphene sheets induce the loss of accessible surface and result in a relatively low specific surface area (SSA) in practical applications.³ In contrast, three-dimensional graphene-assembled monoliths (3D GAs), which have been widely reported, possess structural merits and unique properties inherited from graphene sheets but also higher surface utilization and stronger operability, making them more applicable in real applications than individual graphene sheet. The easiest way to obtain a 3D GA is using a 3D template. With a commercial Ni foam both as the template and the catalyst, Cheng et al. realized the preparation of a 3D GA with controlled microstructure through chemical vapor deposition (CVD).⁴ Various templates, such as anodic aluminum oxide (AAO), MgO, and Cu mesh with 3D structure, have been used in the preparation of 3D GAs.^{5–7} In addition to the CVD method, the self-assembly of graphene oxide (GO), which is easily obtained by the oxidation of graphite and has high dispersibility in an aqueous media, has been well-developed for the construction of 3D GAs because of some advantages, such as low cost, high yield, easy scalability, and adjustability. Several review papers have discussed the structural uniqueness and applications of 3D GAs,^{8–19} but due to the variety of the

preparation methods and the formed structures, there are still many unclear points, especially in the understanding of the assembly process, that become hurdles for further research and applications. Thus, an in-depth discussion of their formation mechanism and structure control is urgently required. In this Perspective, we focus on the key factors involved in the self-assembly process of 3D GAs in solution and their influences on structure adjustment. Moreover, we discuss the possible mechanism that enables the solution-based self-assembly and highlight a promising application of 3D GAs in electrochemical energy storage, which features high volumetric energy density.

Three-dimensional graphene-assembled monoliths possess structural merits and unique properties inherited from graphene sheets but also higher surface utilization and stronger operability, making them more applicable in real applications than individual graphene sheets.

Received: December 16, 2014

Accepted: January 28, 2015

Published: January 28, 2015

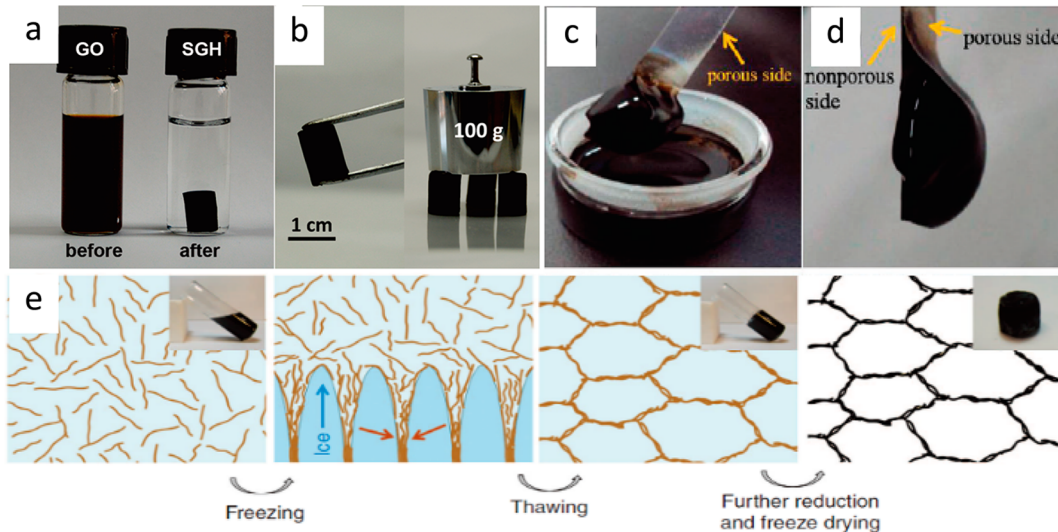


Figure 1. Solution-based self-assembly preparation of 3D GAs. (a) A 2 mg mL^{-1} GO aqueous dispersion before and after hydrothermal reduction. (b) The prepared 3D assembly allowing easy handling and supporting weight.²² Copyright (2010) American Chemical Society. (c) Al^{3+} ions as the linkers promoted assembly of GO on the AAO surface and (d) shows a just take-out fresh hydrogel.³⁷ Copyright (2011) Royal Society of Chemistry. (e) The formation process of the cork-like graphene monolith by a precisely designed freeze-casting.⁴⁰ Copyright (2012) Nature Publishing Group.

Solution-Based Methods for 3D GA Construction. Wang and Ellsworth first reported 3D assembly phenomenon in GO aqueous dispersion. In their study, the self-assembly of GO was observed by increasing the GO concentration or adding a water-soluble polymer like poly(vinyl alcohol) (PVA).²⁰ Various methods have been developed to construct 3D GAs thus far.

Starting with GO, the hydrothermal method is the mostly used method. Wang et al. reported the formation of 3D GAs in the hydrothermal process of GO in the presence of metal ions and glucose, and the metal particles anchored on GO were believed to be the active sites for the assembly.²¹ Shi et al. found that a similar assembly occurred during the hydrothermal process of pure GO dispersion with concentrations higher than 1.0 mg mL^{-1} (Figure 1a and b).²² The hydrothermal process is always accompanied by partial reduction of GO, which is responsible for the assembly formation of 3D GAs.

Such an assembly was also observed in the chemical reduction process of GO.^{23–25} Yan et al. reported that self-assembly of GO was initiated by a mild reduction process at 95°C under atmospheric pressure, where chemical reduction agents, such as NaHSO_3 , Na_2S , vitamin C, HI and hydroquinone, were used.²³ Note that in most of the reduction-induced assembly processes, mild reduction agents are used as strong reduction agents, such as hydrazine, normally cause excessive reduction and prevent the interaction between sheets.²³ However, we found that the assembly can be induced by the reduction of hydrazine with a carefully controlled condition and the assistance of metal ions.²⁵ Even with a thermal reduction at 85°C in the presence of NH_4OH , the assembly of GO is also observed by Worsley et al., and the functional groups serve as chemical cross-linking sites and are transformed into conductive carbon bridges for the assembly.²⁶ Zettl et al. investigated the assembly process and pointed out that the binding of GO sheet was accompanied by a significant loss of oxygen and partial re-formation of the sp^2 carbon network during the assembly process, indicating that the reduction is mainly responsible for the 3D assembly.²⁷ Electrochemical reduction of GO can also realize the formation

of 3D GAs. Shi et al. reported that during the electrochemical reduction process, the reduced GO (rGO) became more hydrophobic and therefore precipitated onto the electrode, forming a 3D porous structure.²⁸

However, in many cases, GO or rGO is hard to assemble into a 3D structure.^{22,29} One of the most possible reasons is that the properties of GO are sensitive to the experimental conditions and the self-assembly of GO only occurs under certain conditions.¹⁷ Thus, the linkers, including polymers, ions, and other small molecules, are used to promote the formation of a 3D GA.^{30–33} Shi et al. found that the assembly of GO in an aqueous solution can be easily initiated by a soluble polymer, PVA, through hydrogen bonding between GO and the hydroxyl moieties of PVA.³⁴ Various polymers that can form hydrogen bonds or are reactive with the functional groups on GO can promote the assembly.^{8,35} It is noted that a cross-linker that reacts with GO can realize the ultrafast assembly. Qiu et al. used an epoxy curing agent with two active primary amine groups, poly(oxypropylene) diamine, to react with the epoxy groups on GO by an opening reaction to realize the assembly of GO within 60 s because of the intercalations of linear diamines with GO.³⁶ We reported a self-assembly of GO at the porous space of AAO, which is initiated by the released Al^{3+} ions that cross-link GO into a hydrogel at the liquid (GO dispersion)—solid (porous AAO) interface (Figure 1c and d).³⁷ Such a cross-linking effect has been reported recently to be crucial in the stabilization of the GO membrane in aqueous media, where multivalent cations cross-link the negatively charged GO.³⁸

Freeze-casting is another important method to fabricate 3D GAs, where the structure can be well controlled by the freezing conditions. During the freezing process, GO or rGO in suspension is rejected from the moving solidification front and piled up between growing cellular solvent crystals, forming the pore walls. This method is not strongly dependent on the starting materials and can be used in many situations. It only relies on the physical interactions for the structure construction.³⁹ Li et al. reported a graphene monolith with a cork-like hierarchical structure fabricated by a precisely designed freeze-casting process of partially reduced GO (Figure

1e). Such a structure has striking mechanical properties because of its biomimetic structure like a natural cork.⁴⁰ This method is also suitable for other dispersible graphene-based materials. Mann et al. produced a graphene–polymer composite with high-order 3D architectures by freeze-casting of homogeneous mixtures of polystyrenesulfonate-stabilized graphene sheets (PSS-G) and PVA. The directional freeze-casting can produce self-supporting high-surface-area monoliths with internally aligned macro- and mesoscale porosity.⁴¹

Another approach for the construction of 3D GAs is with the help of polymerization of organic precursors, which is suitable for GO, rGO, and graphene. Worsley et al. carried out a sol–gel polymerization of resorcinol and formaldehyde with sodium carbonate as a catalyst in an aqueous suspension of GO and obtained a graphene aerogel by simultaneous carbonization of the organic cross-links and thermal reduction of the GO to graphene.⁴² Han et al. demonstrated a typical example of the assembly of Pluronic copolymer functionalized graphene dispersion upon addition of *R*-cyclodextrin (*R*-CD). The Pluronic copolymer not only helps disperse the graphene in aqueous solution but also acts as a reactant to react with *R*-CD for the formation of a 3D graphene-based composite structure.⁴³

Besides the above methods, Seo et al. demonstrated a vacuum centrifugal evaporation method to realize the assembly of GO. At a relatively low temperature (40 °C), GO sheets were assembled into aerogels through van der Waals force due to the dominance of the outward centrifugal force with respect to the upward evaporation force.⁴⁴ Kim et al. developed a simple nucleate boiling approach, which is governed by the dynamics of bubble generation/departure in the graphene colloid solution, for the 3D GA assembly. By adjusting heat flux and boiling time, the 3D GA can be easily formed with the aid of generated bubbles that can be viewed as templates.⁴⁵ These studies suggest that the evaporation control should be another potential strategy to prepare 3D GAs.

Assembly Mechanism. It is easily understood that the freeze-casting method is initiated by the separation of the GO or rGO nanosheet (NS) from the water phase during freezing. The NSs in suspension are rejected from the moving solidification front and concentrated at the boundary of solvent crystals, forming the pore walls, while in the chemical linker-promoted assembly process, GO NSs also need to be separated from the liquid phase because its integration with the linkers greatly reduces the contact of NSs with the solvent. However, other self-assembly processes of GO or rGO in liquid seem more complicated than the above two cases.

A GO or rGO NS can be viewed as a colloid and 2D random diblock copolymer with one graphitic block and another highly oxidized block, which are able to guide molecular assembly through both π – π stacking and hydrogen bonding, respectively.⁴⁶ On the basis of colloidal chemistry, GO can form stable colloidal dispersions because of the strong electrostatic repulsion from the ionization of the oxygen-containing groups, which can overcome the attractive interactions of the van der Waals force from the carbon framework. Besides this, repulsion of hydration and hydrophobic attractive forces exists in the GO and rGO system.⁴⁷ Any route that can shift the balance toward attractive interaction, such as reducing the functional groups or changing the GO–solvent interaction, may help the linkage between the NSs. For example, in a hydrothermal process, the overheated supercritical water can play the role of reducing agent, and the reduction is similar to the H⁺-catalyzed

dehydration of alcohol. This kind of reduction not only partially removes the functional groups on GO but also recovers the aromatic structure of the carbon framework, greatly enhancing the attraction force between the NSs.^{48,49} However, this may not fully explain the formation of the 3D assembly without the help of polymer gelation or templates based on the two fundamental assembly geometries of edge-to-edge and face-to-face. If one only breaks the force balance, such as by decreasing the pH to suppress the ionization of the –COOH groups or by introducing salt ions to destroy the charge balance,^{47,50} no 3D assembly is obtained, and only a precipitate is formed.

A phase separation of GO sheets from a liquid is believed to be responsible for the assembly process, and a continuous liquid phase behaving as the spacer or a continuous template helps form an interlinked pore system and the final 3D network structure.

The reduction causes partial removal of oxygen-containing hydrophilic groups in some regions so that these regions become hydrophobic and cannot disperse in water, resulting in a phase separation at the nanoscale, which generates large sheet deformation as the undispersed regions attach to each other. The hydrophilic regions of the rGO still have a strong interaction with water through hydrogen bonding, which causes some water to adsorb on the rGO surface as a spacer that prevents the parallel aggregation of the sheets,⁵¹ resulting in the final formation of the 3D structure. Other solvents could also act as the spacer for the 3D structure formation as water does, such as propylene carbonate and ionic liquids.^{52,53} From the above discussion, a phase separation of GO sheets from a liquid is believed to be responsible for the assembly process, and a continuous liquid phase behaving as the spacer or a continuous template helps form an interlinked pore system and the final 3D network structure.

As a colloidal system, the assembly of GO or rGO in solution will be greatly affected by its surface chemistry and the concentration, pH, ionic strength, and solvent polarity of the dispersion.⁵⁴ In the following section, the factors responsible for initiating or promoting the assembly process are discussed.

Reduction Process. To realize the phase separation, removing the functional groups by reduction should be the easiest way (Figure 2a), but this also needs the rGO to be dispersible in solution for the assembly process. To achieve this, the reduction degree and process must be controlled to balance the hydrophobicity/hydrophilicity because excessive reduction always induces the precipitation of rGO.⁴⁸ The hydrothermal reduction can be easily tuned by the temperature and time. Higher temperature results in a higher reduction degree, and most of the hydrothermal-process-induced self-assembly occurs above the temperature of 150 °C, indicating that the low reduction degree cannot initiate the self-assembly. We found that the self-assembly did not occur with a very short period of hydrothermal treatment because of the lower reduction degree. For the chemical reduction, the surface chemistry can also be easily tuned by the properties and amount of reduction

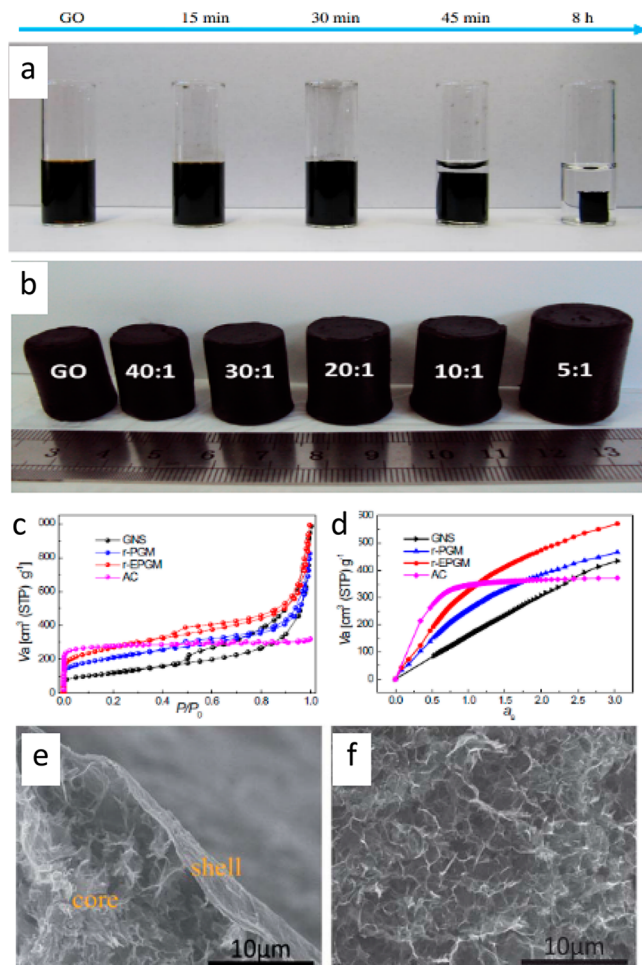


Figure 2. Influences of the reduction process, linker, and impurities on the self-assembly and structure of 3D GA. (a) Photos of GO dispersions after being subjected to reduction by ascorbic acid reduction at 100 °C for different periods of time.⁴⁰ Copyright (2012) Nature Publishing Group. (b) Photographs of graphene-based hydrogels with various GO/PVA weight ratios. It shows that the size of the cylindrical hydrogel increases with increasing PVA fraction. (c) Nitrogen adsorption isotherms of GNS, r-PGM, r-EPGM, and AC. (d) a_s plots of GNS, r-PGM, r-EPGM, and AC.⁶⁸ Copyright (2014) Elsevier. (e,f) SEM images of the typical core–shell structure of the self-assembly of rGO (2 mg mL^{-1}) with the presence of KMnO_4 by reduction of hydrazine.²⁵ Copyright (2011) Royal Society of Chemistry.

agents.^{48,49} Although rGO is still dispersible, a microphase separation has actually occurred as the regions where the oxygen groups have been removed show greatly enhanced hydrophobicity. At the same time, the breaking of epoxy bonds, the evolution of the functional groups, and the restoring of localized π conjugation occur,^{55–57} and these provide opportunities for sheet interactions. However, changes in GO during the reduction process are complicated because of its complex composition. Different reducing agents, such as metal hydrides, ascorbic acid, active metals (e.g., Al, Fe, Cu), ferrous ions, and HI, also cause different reduction degrees and introduce trace noncarbon impurities into the rGO dispersion.⁴⁸ It is claimed that hydrazine both cleans the highly oxidized small fragments attached to GO and removes the oxygen groups bonded to GO.⁵⁸ HI has been proved to be much better than other chemical reduction agents to achieve a

high conductivity of rGO,⁵⁹ and thus, the assembled hydrogel also has a higher conductivity compared with others.²³ However, the influence of reducing agents and these “impurities” on the assembly process are still not well understood.

Solvents. Both GO and rGO can be viewed as kinds of soft materials, and thus, the liquid condition determines their properties.⁵⁴ As mentioned above, the liquid phase should be responsible for the formation of the 3D structure. It also directly affects the separation of GO or rGO because different solvents have different dispersing abilities. In most cases, an aqueous environment is preferable for the assembly process because of the obvious dispersibility changes of GO after reduction. The ionized edges need to be stretched into the bulk solution all of the time; therefore, a conformation of the rGO sheet must occur and results in a curved sheet,¹⁷ providing more chances for intersheet interactions. Qiu et al. found that even with the help of a reactive cross-linker, the assembly of GO does not occur in a pure organic solvent but does in a water/organic mixture.³⁶ A certain nonpolar solvent has no or relatively low dispersing ability for GO, preventing the interaction between NSs because hydrogen bonding interactions preferably occur within the sheet plane.⁸⁰ The adsorption of polar organic solvent molecules such as N-methyl-pyrrolidone (NMP) between two graphene sheets can form an energy barrier,⁶¹ also preventing the interaction between the NSs. For the solvothermal process, the reduction degree should be lower because the reduction process mainly relies on the thermal annealing due to the high boiling point of these solvents, which may be another possible reason for avoiding the linkage of the rGO.^{48,49} Although assembly has also been reported in some organic solvents and ionic liquids, the presence of electrostatic active moieties with GO or rGO is needed.^{43,52,62}

Concentrations. GO or rGO NSs must have a saturation concentration (SC) in dispersions. With the increase of the concentration, the distance between two GO sheets will be decreased, which induces the increase of van der Waals attraction, and when the concentration is higher than SC, the NSs interact with each other and separate from the liquid phase. It is reported that when 20–50 mg of graphite oxide is added in 1 mL of water (much higher than the normal GO concentration), a GO hydrogel is formed after sonication.⁶³ However, there are no reports giving a precise value of the SC because the dispersibility of GO or rGO is largely influenced by its size and surface chemistry. In many cases, such a high concentration is not needed because the assembly processes are mostly promoted by the reduction or adding linkers,^{22,64,65} but a critical concentration is still needed to ensure the full contact and linkage between NSs to form an integrated 3D structure. If the concentration is too low, only a precipitate is obtained,²² which may explain why assembly is not always achieved although similar experimental processes are used.⁶⁶ Normally, the critical concentration is always higher than 1 mg mL^{-1} . According to Shi et al., a low concentration of GO (0.5 mg mL^{-1}) only resulted in precipitation with a hydrothermal treatment, and a weak assembly was formed after the concentration was increased to 1 mg mL^{-1} . A higher concentration also helps increase the mechanical properties of 3D GAs due to the denser structure.²² Besides the mechanical properties, the number and size of the pores can also be tuned, and a low concentration of GO always produces much larger macropores.²¹

Linkers. Adding linkers is the easiest way to realize the linkage of NSs, which simultaneously prevents them from excessive aggregation, resulting in an ultralow density.⁶⁷ It is certain that the addition of linkers will affect the structure of a 3D GA compared with that produced without using linkers. The linkers help the NSs interlock with each other, forming a 3D network with high mechanical resilience.⁶⁷ We investigated the influence of a linker on the structure of a 3D GA by using PVA. The introduction of a small amount of PVA (the mass ratio of GO to PVA is 30:1) results in an apparently larger volume of the resulting hydrogel and a much greater improvement of the SSA from 550 to 750 to 1016 m² g⁻¹ after thermal treatment (denoted r-PGM and r-EPGM for the assembly without and with PVA, respectively), suggesting that PVA acts as a scaffold that prevents the aggregation of rGO NSs (Figure 2b).⁶⁸ The adsorption isotherms of r-EPGMs combine the characters of type-I and -IV isotherms, indicating the existence of a hierarchical pore structure, which is different from the structure of activated carbon (AC, microporous carbon) and randomly aggregated graphene (GNS) without micropores (Figure 2c). Besides, r-EPGM is characterized by more micropores than r-PGM. The α_s plots of r-PGM and r-EPGM lie in between those of AC and GNS, also suggesting the presence of various types of pores (Figure 2d). Various linkers, such as pyrrole and ethylenediamine, can also realize the doping of a 3D GA after thermal treatment.⁶⁹ More importantly, these thermally carbonized linkers serve as carbon cross-linkers in the graphene network, improving the conductivity.⁴²

Heating. It is also noted that temperature is always important in most of the reported assembly processes. For the hydrothermal assembly, the temperature is generally higher than 150 °C, and for chemical reduction-induced assembly, it is higher than 70 °C.^{21–23,25,70} Thermal fluctuation is a driving force for the corrugation of graphene, and increasing temperature could make graphene more corrugated.⁷¹ This also promotes the removal of functional groups, improving the phase separation and the chances for interactions between sheets. Because colloid particles undergo restless Brownian motion in dispersions, the mobility of rGO or GO sheets is also enhanced, leading to faster and closer packing upon heating. This also accelerates the assembly initiated by the reactive linkers because of the faster reaction rate. When using double-stranded DNA (ds-DNA) as the linker, the heating process makes the ds-DNA unwind to bridge adjacent GO sheets by strong noncovalent interactions.⁷²

Sheet Size. Large GO NSs have limited mobility and much more opportunities to contact with each other compared with small sheets.⁵⁴ A high viscosity gel can be formed using only 0.5% (w/w) (5 mg mL⁻¹) of GO NSs with a size up to a few thousand square micrometers.⁷³ Smaller NSs, both for GO and rGO, with a higher edge-to-area ratio are more hydrophilic and more stable in solution due to the decreasing van der Waals attraction. It is found that no gelation occurs for GO sheets smaller than 1 μm even though the concentration is as high as 9 mg mL⁻¹.⁸ Sheet size will also affect the final structure and property. Kim et al. found that the GO papers made of larger GO sheets had significantly higher mechanical properties and electrical conductivity than those with smaller sheets because of the enhanced interaction energy between adjacent GO NSs in different planes.⁷⁴ However, there are few detailed reports of 3D GAs related to the sheet size or aspect ratio. One of the most important reasons is that it is hard to obtain a large amount of GO NSs with similar size. In most cases, the size of

the GO in dispersion obtained by sonication ranges from tens of nanometers to a few micrometers. Although some methods, such as the centrifugal method and pH-induced sieving, can efficiently obtain GO NSs with narrow size distribution, the yield is too low. The lateral size is also greatly influenced by the sonication process,⁷⁵ and the exposed new edges have fewer functional groups to promote assembly formation.⁷⁶ These results also indicate that the differences in preparation process may result in variance of the assembly process and microstructure even with similar size in different studies.

pH. A gellable assembly in acidic media (pH < 7) and a gel-sol transition under alkaline conditions are observed for GO and GO/polymer composites due to the strong repulsion derived from the deprotonated carboxyl groups under alkaline conditions.^{34,63} Besides, under alkaline conditions, the reduction degree can also be increased using HO⁻ as a catalyst.⁷⁷ Other than the electrostatic repulsion forces, the pH leads to a more complicated behavior of GO in solution due to its nonuniform surface chemistry, which affects the dispersibility of GO and rGO with different sizes. In an acidic environment, GO NSs tend to agglomerate to reduce the contact area between hydrophobic regions and water, while an intrasheet contraction or folding is favorable in alkaline conditions.⁷⁸ It is shown that freeze-casting of rGO results in the formation of a 3D porous graphene foam with pH < 8 and nanoscrolls with pH = 10 because the carboxylic groups at the edges are deprotonated at the pH of 10.⁷⁹

Ions and Impurities. The introduction of metal ions promotes the formation of a 3D structure because of the chemical adsorption of these ions on GO sheets.^{21,30,80} The ions are also introduced during the reduction by activated metals, and ferrous ions are believed to promote the assembly and affect the resulting structure.^{31,81} However, no detailed study has been conducted to clarify the effect of ions on the resulting structure. In a previous study, we investigated the influence of ions by introducing KMnO₄ to the GO dispersion during the reduction by hydrazine hydrate and obtained an assembly with a core-shell structure (Figure 2e and f), suggesting that the metal ions affect the assembly process and the final structure. With a decrease of the KMnO₄ content, the pore structure becomes loosened, and the obtained assembly has a larger size. Although the mechanism has not been fully understood, it clearly shows that the ions and impurities have large influences on the assembly process and the final structure.⁸⁵

Template. The easiest way to control the structure is to use a template. The most common hard template is ice in the freeze-casting, and this greatly depends on the freezing conditions. Li et al. reported a cellular structure with superelasticity prepared by carefully controlling the freezing process and the resulting ice template.⁴⁰ Besides this, many organic droplets can also be used as templates. Because GO is an amphiphile that can act as a surfactant that adsorbs on interfaces, it can stabilize oil or organic droplets in an aqueous condition.^{82,83} Using this feature, Shi et al. used organic droplets (hexane) as templates and also obtained a cellular structure.⁸⁴ During the hydrothermal process, GO NSs were reduced to rGO and formed a well-defined and interconnected 3D network around the hexane droplets. Thus, hexane droplets can be viewed as soft templates with the diameters in the range of several tens of micrometers to about 200 μm and help form macroporous structures in 3D GAs. Considering the size-dependent amphiphilic properties of GO, the emulsion and the size of the droplet will be largely affected by the size of the GO, which

will have a great influence on the final structure.⁴⁶ These two kinds of templates, ice as the hard template and a droplet as the soft template, can also be used at same time. Together with the nanosized “soft” droplets in the liquid phase, the roughness of the microsized “hard” ice template contributes to the formation of a combination of microporous and nanoporous structures.⁸⁵ Various materials, such as PS spheres, SiO₂ nanoparticles, and surfactant molecules, have been used as a shaping template to control the structure of graphene-based materials,^{86–89} and these can also be introduced in the assembly process to tune the structure of the 3D GAs.

Controlling the drying process is a simple but effective way to simultaneously tailor the structures and properties of 3D GA, such as pore structure, density, mechanical strength, conductivity and so on.

Drying Method. Strong hydrogen bonding and capillary compression forces exist between the NS and H₂O,^{51,60} and thus, the freeze-drying method is always used to maintain the shape and the microstructure of a just-obtained wet assembly to avoid the aggregation of the NSs. Although supercritical drying can also be used to fix the structure, it is rarely used because of its high cost and complexity. These drying methods always bring low density and poor mechanical properties for the assembly without the help of linkers.⁹⁰ In a dramatically opposite way, we used slow evaporation to replace the freeze-drying process and obtained a new highly dense but porous carbon (Figure 3a). Unlike the 3D structures with very low density (PGM) obtained by freeze-drying, this carbon (HPGM) has a high density of 1.58 g cm⁻³, which is 70% of the density of graphite, but it still has a high SSA of 367 m² g⁻¹

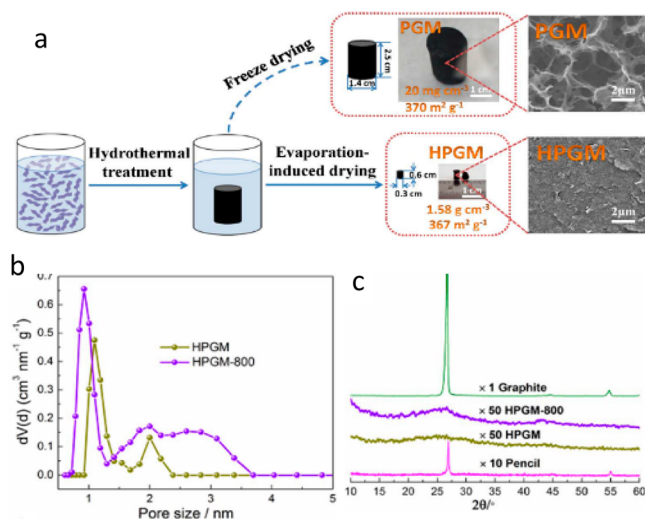


Figure 3. High-density but porous 3D GA obtained by slow evaporation drying. (a) Schematic of the formation of 3D GAs with different drying processes and the SEM images of the resultant PGM and HPGM; (b) pore size distributions (DFT) of HPGM and HPGM-800; (c) XRD patterns of graphite, soft pencil lead, HPGM, and HPGM-800.⁹¹ Copyright (2013) Nature Publishing Group.

and an interconnected pore structure.⁹¹ In the evaporation-induced drying, the evaporation of water exerts a “pulling force” on the graphene layers and results in the shrinkage of the 3D network because of the capillary compression. Unexpectedly, the high-density GA retains an interconnected porous structure that consists of small cylindrical pores less than 2 nm (Figure 3b). As demonstrated by the X-ray diffraction (XRD) patterns, the arrangement of the graphene NSs (no layering structure) in the GA is totally different from that of graphite or graphite products (like pencils), suggesting that highly wrinkled NSs are interlinked with each other to form a porous structure in a disordered but highly compact way (Figure 3c). The increase of the density can bring higher electrical conductivity, and under alkaline condition, a more solid structure and higher density will be reached, resulting in better compressive strength.⁹² Such a structure also has isotropic electrical conductivities and Young’s moduli properties, which are much higher than isotropic graphite but with a much simpler preparation method.⁹³

On the basis of the water phase diagram, we also proposed a two-stage drying process to replace the generally used slow evaporation for the preparation of a graphene membrane.^{94–96} With a reduced pressure, the water trapped in the wet membrane boils violently and then instantaneously transforms into ice crystals around the triple point, and this provides strong forces to change and fix the microstructure of membrane. This membrane has a 3D graded structure (Figure 4a–d) and shows high surface utilization compared to the compact membrane obtained by normal drying.⁹⁷ Note that such a graded structure can only be obtained in a membrane assembled at the liquid/air interface because the originally

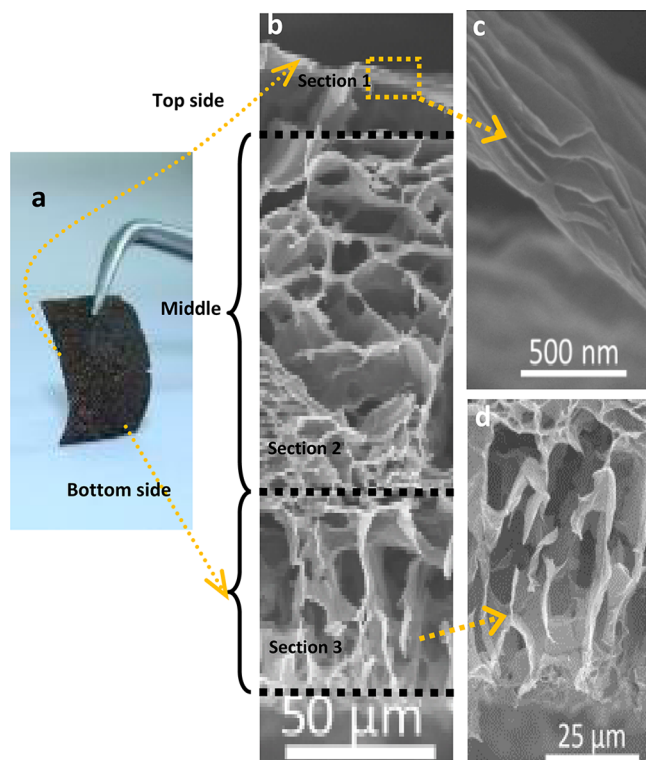


Figure 4. Graded structure of a GO membrane prepared by a two-stage drying process. (a) Photograph of a membrane with a graded structure; (b–d) cross-sectional SEM images of the membrane.⁹⁷ Copyright (2014) Wiley-VCH.

formed part (top) of the membrane (Figure 4a and b), which was exposed to air, gradually dried, forming a tightly layered structure that helps maintain and fix the membrane morphology during the following two-stage drying process. The above discoveries provide a new strategy to tailor the microstructure of a 3D GA by controlling the drying process for different applications.

External Forces. A liquid crystal is the mesomorphic ordered state of anisotropic particles that is also observed from the GO dispersions. The GO NSs in the freeze-dried liquid crystal are smoothly bent along a specific orientation. More importantly, the orientation of GO liquid crystals could be manipulated by a magnetic or electric field or mechanical deformation, which may be used to tune the structure of the GO assemblies and is worthy of detailed investigation.⁹⁸

3D GAs hold potentials in the electrochemical energy storage especially featuring high rate and high volumetric energy density.

Applications. 3D GAs have been widely explored for applications in the fields of energy storage and conversion, environmental protection, and biochemical and biomedical related systems because of their high SSA and unique pore structure. They can be used as a biocompatible and conductive scaffold for neural stem cells or used to capture the cancer cells.^{99,100} These materials also show large adsorption capacities for organic pollutants, oils, heavy metal ions, and toxic gases and can be easily recycled due to their good mechanical strength and thermal stability.^{101,102} Graphene can be used as a template to shape the formation of other components,^{103–105} and thus, a 3D GA can be used as a 3D template and can be easily removed by calcination or the reaction with other components, such as preparing porous MnO₂ by the oxidation reaction of KMnO₄ with GA.¹⁰⁶ Besides the above-mentioned cases, the most promising applications are in the electrochemical-related fields because of the continuous conducting and mass transportation network formed by the interlinked graphene sheets and pores.¹⁰⁷ 3D GAs and their hybrids have been investigated in Li ion batteries, Li–air batteries, Li–S batteries, and supercapacitors and used for capacitive deionization.^{107–112} More importantly, the assemblies can be directly pressed into an electrode and, thus, do not need a current collector or additives, helping improve the energy density based on the devices.¹¹³ Details of their applications can be found in recent review articles,^{8–19} and here, we emphasize one of the focal points for their future electrochemical applications.

The biggest drawback of nanomaterials is their low density, which results in a low volumetric energy density and limits their practical applications in energy storage. Li et al. prepared a porous yet densely packed carbon electrode by capillary compression of adaptive graphene gel films in the presence of a nonvolatile liquid electrolyte. The packing density can be increased to 1.33 g cm⁻³, and the volumetric energy density approaches 60 W h L⁻¹.¹¹⁴ However, how to achieve a highly compact graphene assembly while retaining a high porosity is still a challenge. As mentioned above, we reported the formation of a novel close-grained HPGM with high density that balances these two opposing characteristics using evaporation-induced drying. This carbon has a porous microstructure and a large density (up to 1.58 g cm⁻³) and therefore

is a potentially ideal electrode material with high volumetric capacitance (up to 376 F cm⁻³; Figure 5a).⁹¹ Both freeze-dried

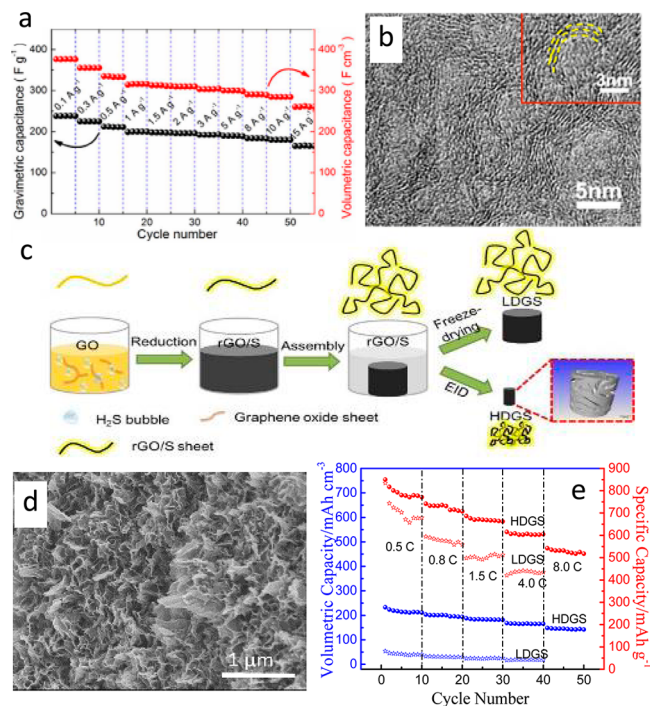


Figure 5. High volumetric energy storage performance of 3D GA-based materials. (a) The electrochemical performance of HPGM in an aqueous system (6 M KOH) and (b) TEM image of the HPGM showing the interlinked structure.⁹¹ Copyright (2013) Nature Publishing Group. (c) Illustration of the formation of high-density graphene/sulfur hybrid (HDGS) using the evaporation drying method. (d,e) SEM image and electrochemical performance of HDGS and the freeze-dried low-density hybrid (LDGS).¹¹⁵ Copyright (2015) Royal Society of Chemistry.

PGM and HPGM show similar gravimetric capacitance in the aqueous system, but PGM has a very limited volumetric capacitance (lower than 10 F cm⁻³). HPGM also shows a very good rate capability that retains 69% of the maximum capacitance at a high current density of 15 A g⁻¹. The excellent rate performance can be ascribed to the interlinked graphene NSs that guarantee fast electron transfer and ion transport (Figure 5b). Moreover, we have extended the slow evaporation-induced structure control for this high-density material to the preparation of hybrid materials with high density. For example, we demonstrated a high-density graphene/sulfur hybrid (HDGS) by combining the predeposition of sulfur on GO NSs and a reduction-promoted assembly process (Figure 5c and d). A volumetric capacity of 233 mA h cm⁻³ at 0.5 C was obtained, which still reached about 149 mA h cm⁻³ with the current density of 8 C (capacity retention of 64%), illustrating a high volumetric capacity and excellent rate performance (Figure 5e).¹¹⁵ The above studies suggest that the assembly of graphene is a very promising way to realize real applications of graphene-based materials and prepare novel carbon materials with well-designed structure.

Outlook. To pave the way for the future applications of 3D GAs, there is still much work to do, and several key issues need to be solved. First, in-depth understanding of the specific mechanism of each assembly method is important at this stage, not only for realizing full control of the assembly process and

microstructure of 3D GAs but also for clarifying common points (intersheet interaction) across different assemblies. Phase separation and liquid spacers should be crucial for the 3D assembly of GO or rGO in various cases, but more experimental evidence and much clearer theoretical explanations are needed to have a very reasonable understanding of the assembly. The properties of the GO precursor are sensitive to the experimental conditions, resulting in big differences in sheet size and shape, thickness, surface chemistry and defects and traces of impurities, which greatly affect the interactions between GO or rGO in different studies. Thus, even with the same assembly method, the exhibited phenomena and structures are different from each other, which hinders the understanding of the assembly process. Thus, the second issue is developing an effective way to precisely control the structure of the starting GO and clarify its role in different assembly environments, which is a precondition for a well-controlled assembly process and microstructure. Lastly but most importantly, 3D GA is not only a promising form for graphene application but also regarded as a new class of carbon material artificially built with graphene blocks that may exist either as the lightest carbon foam or as a highly dense but porous carbon. Graphene renews our understandings of carbon allotropes, while graphene assemblies renew our understanding of carbon materials, which are awaiting our new insights to the structure, properties, and performance of carbon materials, and, more importantly, scale up preparation and industrial applications of graphene and graphene assemblies.

AUTHOR INFORMATION

Corresponding Author

*E-mail: qhyangcn@tju.edu.cn and yang.quanhong@sz.tsinghua.edu.cn.

Notes

The authors declare no competing financial interest.

Biographies

Wei Lv received his Ph.D. from Tianjin University in 2012. He currently works as a postdoctoral researcher at the Graduate School at Shenzhen, Tsinghua University. His research mainly focuses on graphene assemblies and their applications in electrochemical sensing and energy storage.

Chen Zhang received his B.S. degree from Tianjin University in 2010 and continued his study as a doctoral candidate at the same university under the supervision of Prof. Quan-Hong Yang. His research includes the design and controlled preparation of graphene-based materials for compact energy storage devices.

Zhengjie Li received his B.S. degree from China University of Mining & Technology (Beijing) in 2011 and is currently a doctoral candidate under the supervision of Prof. Quan-Hong Yang at Tianjin University. His current research interests are focused on the preparation and application of novel materials using graphene templates.

Quan-Hong Yang joined Tianjin University as a full professor of nanomaterials in 2006 and is leading a joint graphene lab of Tianjin University and the Graduate School at Shenzhen, Tsinghua University. His research focuses on novel carbon materials with their applications in energy storage and environmental protection. See <http://nanoyang.tju.edu.cn> for more details.

ACKNOWLEDGMENTS

National Basic Research Program of China (2014CB932400), National Natural Science Foundation of China (Nos.

U1401243, 51372167, and 51302146), NSAF (U1330123), Shenzhen Basic Research Project (JCYJ20130402145002430 and ZDSYS20140509172959981), and China Postdoctoral Science Foundation (2013T60111). We also thank the financial support from the Guangdong Province Innovation R&D Team Plan (No. 2009010025).

REFERENCES

- (1) Novoselov, K. S.; Fal'ko, V. I.; Colombo, L.; Gellert, P. R.; Schwab, M. G.; Kim, K. A Roadmap for Graphene. *Nature* **2012**, *490*, 192–200.
- (2) Yang, Q. H.; Lu, W.; Yang, Y. G.; Wang, M. Z. Free Two-Dimensional Carbon Crystal — Single-Layer Graphene. *New Carbon Mater.* **2008**, *23*, 97–103.
- (3) Luo, J. Y.; Kim, J.; Huang, J. X. Material Processing of Chemically Modified Graphene: Some Challenges and Solutions. *Acc. Chem. Res.* **2013**, *46*, 2225–2234.
- (4) Chen, Z. P.; Ren, W. C.; Gao, L. B.; Liu, B. L.; Pei, S. F.; Cheng, H. M. Three-Dimensional Flexible and Conductive Interconnected Graphene Networks Grown by Chemical Vapour Deposition. *Nat. Mater.* **2011**, *10*, 424–428.
- (5) Zeng, Z. Y.; Huang, X.; Yin, Z. Y.; Li, H.; Chen, Y.; Li, H.; Zhang, Q.; Ma, J.; Boey, F.; Zhang, H. Fabrication of Graphene Nanomesh by Using an Anodic Aluminum Oxide Membrane as a Template. *Adv. Mater.* **2012**, *24*, 4138–4142.
- (6) Li, X.; Sun, P. Z.; Fan, L. L.; Zhu, M.; Wang, K. L.; Zhong, M. L.; Wei, J. Q.; Wu, D. H.; Cheng, Y.; Zhu, H. W. Multifunctional Graphene Woven Fabrics. *Sci. Rep.* **2012**, *2*, 395.
- (7) Ma, Y.; Chen, Y. Three-Dimensional Graphene Networks: Synthesis, Properties and Applications. *Natl. Sci. Rev.* **2014**, DOI: 10.1093/nsr/nwu072.
- (8) Li, C.; Shi, G. Q. Functional Gels Based on Chemically Modified Graphenes. *Adv. Mater.* **2014**, *26*, 3992–4012.
- (9) Chabot, V.; Higgins, D.; Yu, A. P.; Xiao, X. C.; Chen, Z. W.; Zhang, J. J. A Review of Graphene and Graphene Oxide Sponge: Material Synthesis and Applications to Energy and the Environment. *Energy Environ. Sci.* **2014**, *7*, 1564–1596.
- (10) Yin, S. Y.; Niu, Z. Q.; Chen, X. D. Assembly of Graphene Sheets into 3D Macroscopic Structures. *Small* **2012**, *8*, 2458–2463.
- (11) Nardeccchia, S.; Carriazo, D.; Ferrer, M. L.; Gutierrez, M. C.; del Monte, F. Three Dimensional Macroporous Architectures and Aerogels Built of Carbon Nanotubes and/or Graphene: Synthesis and Applications. *Chem. Soc. Rev.* **2013**, *42*, 794–830.
- (12) Li, C.; Shi, G. Q. Three-Dimensional Graphene Architectures. *Nanoscale* **2012**, *4*, 5549–5563.
- (13) Zhou, G. J.; Ye, Z. K.; Shi, W. W.; Liu, J. Y.; Xi, F. N. Applications of Three Dimensional Graphene and Its Composite Materials. *Prog. Chem.* **2014**, *26*, 950–960.
- (14) Cao, X. H.; Yin, Z. Y.; Zhang, H. Three-Dimensional Graphene Materials: Preparation, Structures and Application in Supercapacitors. *Energy Environ. Sci.* **2014**, *7*, 1850–1865.
- (15) Zhao, Z. F.; Wang, X. B.; Qiu, J. L.; Lin, J. J.; Xu, D. D.; Zhang, C.; Lv, M. J.; Yang, X. Y. Three-Dimensional Graphene-Based Hydrogel/Aerogel Materials. *Rev. Adv. Mater. Sci.* **2014**, *36*, 137–151.
- (16) Lv, R. T.; Cruz-Silva, E.; Terrones, M. Building Complex Hybrid Carbon Architectures by Covalent Interconnections: Graphene–Nanotube Hybrids and More. *ACS Nano* **2014**, *8*, 4061–4069.
- (17) Whitby, R. L. D. Chemical Control of Graphene Architecture: Tailoring Shape and Properties. *ACS Nano* **2014**, *8*, 9733–9754.
- (18) Xu, Y. X.; Shi, G. Q. Assembly of Chemically Modified Graphene: Methods and Applications. *J. Mater. Chem.* **2011**, *21*, 3311–3323.
- (19) Shao, J. J.; Lv, W.; Yang, Q. H. Self-Assembly of Graphene Oxide at Interfaces. *Adv. Mater.* **2014**, *26*, 5586–5612.
- (20) Wang, J.; Ellsworth, M. W. Graphene Aerogels. *ECS Trans.* **2009**, *19*, 241–247.

- (21) Tang, Z. H.; Shen, S. L.; Zhuang, J.; Wang, X. Noble-Metal-Promoted Three-Dimensional Macroassembly of Single-Layered Graphene Oxide. *Angew. Chem., Int. Ed.* **2010**, *49*, 4603–4607.
- (22) Xu, Y. X.; Sheng, K. X.; Li, C.; Shi, G. Q. Self-Assembled Graphene Hydrogel via a One-Step Hydrothermal Process. *ACS Nano* **2010**, *4*, 4324–4330.
- (23) Chen, W. F.; Yan, L. F. In Situ Self-Assembly of Mild Chemical Reduction Graphene for Three-Dimensional Architectures. *Nanoscale* **2011**, *3*, 3132–3137.
- (24) Hu, C. G.; Zhai, X. Q.; Liu, L. L.; Zhao, Y.; Jiang, L.; Qu, L. T. Spontaneous Reduction and Assembly of Graphene Oxide into Three-Dimensional Graphene Network on Arbitrary Conductive Substrates. *Sci. Rep.* **2013**, *3*, 2065.
- (25) Lv, W.; Tao, Y.; Ni, W.; Zhou, Z.; Su, F. Y.; Chen, X. C.; Jin, F. M.; Yang, Q. H. One-Pot Self-Assembly of Three-Dimensional Graphene Macroassemblies with Porous Core and Layered Shell. *J. Mater. Chem.* **2011**, *21*, 12352–12357.
- (26) Worsley, M. A.; Kucheyev, S. O.; Mason, H. E.; Merrill, M. D.; Mayer, B. P.; Lewicki, J.; Valdez, C. A.; Suss, M. E.; Stadermann, M.; Pauzauskie, P. J.; et al. Mechanically Robust 3D Graphene Macroassembly with High Surface Area. *Chem. Commun.* **2012**, *48*, 8428–8430.
- (27) Goldstein, A. P.; Mickelson, W.; Machness, A.; Lee, G.; Worsley, M. A.; Woo, L.; Zettl, A. Simultaneous Sheet Cross-Linking and Deoxygenation in the Graphene Oxide Sol–Gel Transition. *J. Phys. Chem. C* **2014**, *118*, 28855–28860.
- (28) Sheng, K. X.; Sun, Y. Q.; Li, C.; Yuan, W. J.; Shi, G. Q. Ultrahigh-Rate Supercapacitors Based on Electrochemically Reduced Graphene Oxide for AC Line-Filtering. *Sci. Rep.* **2012**, *2*, 247.
- (29) Chen, C. B.; Li, J.; Li, R.; Xiao, G. Y.; Yan, D. Y. Synthesis of Superior Dispersions of Reduced Graphene Oxide. *New J. Chem.* **2013**, *37*, 2778–2783.
- (30) Jiang, X.; Ma, Y. W.; Li, J. J.; Fan, Q. L.; Huang, W. Self-Assembly of Reduced Graphene Oxide into Three-Dimensional Architecture by Divalent Ion Linkage. *J. Phys. Chem. C* **2010**, *114*, 22462–22465.
- (31) Cong, H. P.; Ren, X. C.; Wang, P.; Yu, S. H. Macroscopic Multifunctional Graphene-Based Hydrogels and Aerogels by a Metal Ion Induced Self-Assembly Process. *ACS Nano* **2012**, *6*, 2693–2703.
- (32) Bai, H.; Li, C.; Wang, X. L.; Shi, G. Q. On the Gelation of Graphene Oxide. *J. Phys. Chem. C* **2011**, *115*, 5545–5551.
- (33) Sudeep, P. M.; Narayanan, T. N.; Ganesan, A.; Shajumon, M. M.; Yang, H.; Ozden, S.; Patra, P. K.; Pasquali, M.; Vajtai, R.; Ganguli, S.; et al. Covalently Interconnected Three-Dimensional Graphene Oxide Solids. *ACS Nano* **2013**, *7*, 7034–7040.
- (34) Bai, H.; Li, C.; Wang, X. L.; Shi, G. Q. A pH-Sensitive Graphene Oxide Composite Hydrogel. *Chem. Commun.* **2010**, *46*, 2376–2378.
- (35) Tao, C. A.; Wang, J. F.; Qin, S. Q.; Lv, Y. A.; Long, Y.; Zhu, H.; Jiang, Z. H. Fabrication of pH-Sensitive Graphene Oxide–Drug Supramolecular Hydrogels as Controlled Release Systems. *J. Mater. Chem.* **2012**, *22*, 24856–24861.
- (36) Wan, W. B.; Li, L. L.; Zhao, Z. B.; Hu, H.; Hao, X. J.; Winkler, D. A.; Xi, L. C.; Hughes, T. C.; Qiu, J. S. Ultrafast Fabrication of Covalently Cross-Linked Multifunctional Graphene Oxide Monoliths. *Adv. Funct. Mater.* **2014**, *24*, 4915–4921.
- (37) Shao, J. J.; Wu, S. D.; Zhang, S. B.; Lv, W.; Su, F. Y.; Yang, Q. H. Graphene Oxide Hydrogel at Solid/Liquid Interface. *Chem. Commun.* **2011**, *47*, 5771–5773.
- (38) Yeh, C. N.; Raidongia, K.; Shao, J. J.; Yang, Q. H.; Huang, J. X. On the Origin of the Stability of Graphene-Oxide Membranes in Water. *Nat. Chem.* **2015**, DOI: 10.1038/nchem.2145.
- (39) Deville, S. Freeze-Casting of Porous Ceramics: A Review of Current Achievements and Issues. *Adv. Eng. Mater.* **2008**, *10*, 155–169.
- (40) Qiu, L.; Liu, J. Z.; Chang, S. L. Y.; Wu, Y. Z.; Li, D. Biomimetic Superelastic Graphene-Based Cellular Monoliths. *Nat. Commun.* **2012**, *3*, 1241.
- (41) Vickery, J. L.; Patil, A. J.; Mann, S. Fabrication of Graphene–Polymer Nanocomposites with Higher-Order Three-Dimensional Architectures. *Adv. Mater.* **2009**, *21*, 2180–2184.
- (42) Worsley, M. A.; Pauzauskie, P. J.; Olson, T. Y.; Biener, J.; Satcher, J. H.; Baumann, T. F. Synthesis of Graphene Aerogel with High Electrical Conductivity. *J. Am. Chem. Soc.* **2010**, *132*, 14067–14069.
- (43) Zu, S. Z.; Han, B. H. Aqueous Dispersion of Graphene Sheets Stabilized by Pluronic Copolymers: Formation of Supramolecular Hydrogel. *J. Phys. Chem. C* **2009**, *113*, 13651–13657.
- (44) Liu, F.; Seo, T. S. A Controllable Self-Assembly Method for Large-Scale Synthesis of Graphene Sponges and Free-Standing Graphene Films. *Adv. Funct. Mater.* **2010**, *20*, 1930–1936.
- (45) Ahn, H. S.; Jang, J. W.; Seol, M.; Kim, J. M.; Yun, D. J.; Park, C.; Kim, H.; Youn, D. H.; Kim, J. Y.; Park, G.; et al. Self-Assembled Foam-Like Graphene Networks Formed through Nucleate Boiling. *Sci. Rep.* **2013**, *3*, 1396.
- (46) Kim, J.; Cote, L. J.; Huang, J. X. Two Dimensional Soft Material: New Faces of Graphene Oxide. *Acc. Chem. Res.* **2012**, *45*, 1356–1364.
- (47) Li, D.; Muller, M. B.; Gilje, S.; Kaner, R. B.; Wallace, G. G. Processable Aqueous Dispersions of Graphene Nanosheets. *Nat. Nanotechnol.* **2008**, *3*, 101–105.
- (48) Pei, S. F.; Cheng, H. M. The Reduction of Graphene Oxide. *Carbon* **2012**, *50*, 3210–3228.
- (49) Chua, C. K.; Pumera, M. Chemical Reduction of Graphene Oxide: A Synthetic Chemistry Viewpoint. *Chem. Soc. Rev.* **2014**, *43*, 291–312.
- (50) Shih, C. J.; Lin, S. C.; Sharma, R.; Strano, M. S.; Blankschtein, D. Understanding the pH-Dependent Behavior of Graphene Oxide Aqueous Solutions: A Comparative Experimental and Molecular Dynamics Simulation Study. *Langmuir* **2012**, *28*, 235–241.
- (51) Yang, X. W.; Zhu, J. W.; Qiu, L.; Li, D. Bioinspired Effective Prevention of Restacking in Multilayered Graphene Films: Towards the Next Generation of High-Performance Supercapacitors. *Adv. Mater.* **2011**, *23*, 2833–2838.
- (52) Srinivasan, S.; Shin, W. H.; Choi, J. W.; Coskun, A. A Bifunctional Approach for the Preparation of Graphene and Ionic Liquid-Based Hybrid Gels. *J. Mater. Chem. A* **2013**, *1*, 43–48.
- (53) Sun, Y. Q.; Wu, Q.; Shi, G. Q. Supercapacitors Based on Self-Assembled Graphene Organogel. *Phys. Chem. Chem. Phys.* **2011**, *13*, 17249–17254.
- (54) Cheng, C.; Li, D. Solvated Graphenes: An Emerging Class of Functional Soft Materials. *Adv. Mater.* **2013**, *25*, 13–30.
- (55) Gao, W.; Alemany, L. B.; Ci, L. J.; Ajayan, P. M. New Insights into the Structure and Reduction of Graphite Oxide. *Nat. Chem.* **2009**, *1*, 403–408.
- (56) Bagri, A.; Mattevi, C.; Acik, M.; Chabal, Y. J.; Chhowalla, M.; Shenoy, V. B. Structural Evolution During the Reduction of Chemically Derived Graphene Oxide. *Nat. Chem.* **2010**, *2*, 581–587.
- (57) Choudhary, S.; Mungse, H. P.; Khatri, O. P. Hydrothermal Deoxygenation of Graphene Oxide: Chemical and Structural Evolution. *Chem.—Asian J.* **2013**, *8*, 2070–2078.
- (58) Thomas, H. R.; Day, S. P.; Woodruff, W. E.; Valles, C.; Young, R. J.; Kinloch, I. A.; Morley, G. W.; Hanna, J. V.; Wilson, N. R.; Rourke, J. P. Deoxygenation of Graphene Oxide: Reduction or Cleaning? *Chem. Mater.* **2013**, *25*, 3580–3588.
- (59) Pei, S. F.; Zhao, J. P.; Du, J. H.; Ren, W. C.; Cheng, H. M. Direct Reduction of Graphene Oxide Films into Highly Conductive and Flexible Graphene Films by Hydrohalic Acids. *Carbon* **2010**, *48*, 4466–4474.
- (60) Yoon, Y.; Lee, K.; Baik, C.; Yoo, H.; Min, M.; Park, Y.; Lee, S. M.; Lee, H. Anti-Solvent Derived Non-Stacked Reduced Graphene Oxide for High Performance Supercapacitors. *Adv. Mater.* **2013**, *25*, 4437–4444.
- (61) Shih, C. J.; Lin, S. C.; Strano, M. S.; Blankschtein, D. Understanding the Stabilization of Liquid-Phase-Exfoliated Graphene in Polar Solvents: Molecular Dynamics Simulations and Kinetic Theory of Colloid Aggregation. *J. Am. Chem. Soc.* **2010**, *132*, 14638–14648.

- (62) Gun, J.; Kulkarni, S. A.; Xiu, W.; Batabyal, S. K.; Sladkevich, S.; Prikhodchenko, P. V.; Gutkin, V.; Lev, O. Graphene Oxide Organogel Electrolyte for Quasi Solid Dye Sensitized Solar Cells. *Electrochim. Commun.* **2012**, *19*, 108–110.
- (63) Qin, S. Y.; Liu, X. J.; Zhuo, R. X.; Zhang, X. Z. Microstructure-Controllable Graphene Oxide Hydrogel Film Based on a pH-Responsive Graphene Oxide Hydrogel. *Macromol. Chem. Phys.* **2012**, *213*, 2044–2051.
- (64) Worsley, M. A.; Pham, T. T.; Yan, A. M.; Shin, S. J.; Lee, J. R. I.; Bagge-Hansen, M.; Mickelson, W.; Zettl, A. Synthesis and Characterization of Highly Crystalline Graphene Aerogels. *ACS Nano* **2014**, *8*, 11013–11022.
- (65) Goldstein, A. P.; Mickelson, W.; Machness, A.; Lee, G.; Worsley, M. A.; Woo, L.; Zettl, A. Simultaneous Sheet Cross-Linking and Deoxygenation in the Graphene Oxide Sol–Gel Transition. *J. Phys. Chem. C* **2014**, *118*, 28855–28860.
- (66) Zhou, Y.; Bao, Q. L.; Tang, L. A. L.; Zhong, Y. L.; Loh, K. P. Hydrothermal Dehydration for the “Green” Reduction of Exfoliated Graphene Oxide to Graphene and Demonstration of Tunable Optical Limiting Properties. *Chem. Mater.* **2009**, *21*, 2950–2956.
- (67) Hu, H.; Zhao, Z. B.; Wan, W. B.; Gogotsi, Y.; Qiu, J. S. Ultralight and Highly Compressible Graphene Aerogels. *Adv. Mater.* **2013**, *25*, 2219–2223.
- (68) Tao, Y.; Kong, D. B.; Zhang, C.; Lv, W.; Wang, M. X.; Li, B. H.; Huang, Z. H.; Kang, F. Y.; Yang, Q. H. Monolithic Carbons with Spheroidal and Hierarchical Pores Produced by the Linkage of Functionalized Graphene Sheets. *Carbon* **2014**, *69*, 169–177.
- (69) Zhao, Y.; Hu, C. G.; Hu, Y.; Cheng, H. H.; Shi, G. Q.; Qu, L. T. A Versatile, Ultralight, Nitrogen-Doped Graphene Framework. *Angew. Chem. Int. Ed.* **2012**, *51*, 11371–11375.
- (70) Shi, J. L.; Du, W. C.; Yin, Y. X.; Guo, Y. G.; Wan, L. J. Hydrothermal Reduction of Three-Dimensional Graphene Oxide for Binder-Free Flexible Supercapacitors. *J. Mater. Chem. A* **2014**, *2*, 10830–10834.
- (71) Qiu, L.; Zhang, X. H.; Yang, W. R.; Wang, Y. F.; Simon, G. P.; Li, D. Controllable Corrugation of Chemically Converted Graphene Sheets in Water and Potential Application for Nanofiltration. *Chem. Commun.* **2011**, *47*, 5810–5812.
- (72) Xu, Y. X.; Wu, Q. O.; Sun, Y. Q.; Bai, H.; Shi, G. Q. Three-Dimensional Self-Assembly of Graphene Oxide and DNA into Multifunctional Hydrogels. *ACS Nano* **2010**, *4*, 7358–7362.
- (73) Luo, Z. T.; Lu, Y.; Somers, L. A.; Johnson, A. T. C. High Yield Preparation of Macroscopic Graphene Oxide Membranes. *J. Am. Chem. Soc.* **2009**, *131*, 898–899.
- (74) Lin, X. Y.; Shen, X.; Zheng, Q. B.; Yousefi, N.; Ye, L.; Mai, Y. W.; Kim, J. K. Fabrication of Highly-Aligned, Conductive, and Strong Graphene Papers Using Ultra Large Graphene Oxide Sheets. *ACS Nano* **2012**, *6*, 10708–10719.
- (75) Sierra, U.; Álvarez, P.; Santamaría, R.; Granda, M.; Blanco, C.; Menéndez, R. A Multi-Step Exfoliation Approach to Maintain the Lateral Size of Graphene Oxide Sheets. *Carbon* **2014**, *80*, 830–832.
- (76) Compton, O. C.; An, Z.; Putz, K. W.; Hong, B. J.; Hauser, B. G.; Brinson, L. C.; Nguyen, S. T. Additive-Free Hydrogelation of Graphene Oxide by Ultrasonication. *Carbon* **2012**, *50*, 3399–3406.
- (77) Guoan, T.; Tian, Z.; Hongxiang, L.; Jinsong, L.; Jizhou, K.; Fuyong, L. Temperature and pH Effect on Reduction of Graphene Oxides in Aqueous Solution. *Mater. Res. Express* **2014**, *1*, 035605.
- (78) Whitby, R. L. D.; Korobeinyk, A.; Gun’ko, V. M.; Busquets, R.; Cundy, A. B.; Laszlo, K.; Skubiszewska-Zieba, J.; Leboda, R.; Tombacz, E.; Toth, I. Y.; et al. pH-Driven Physicochemical Conformational Changes of Single-Layer Graphene Oxide. *Chem. Commun.* **2011**, *47*, 9645–9647.
- (79) Shin, Y. E.; Sa, Y. J.; Park, S.; Lee, J.; Shin, K. H.; Joo, S. H.; Ko, H. An Ice-Templated, pH-Tunable Self-Assembly Route to Hierarchically Porous Graphene Nanoscroll Networks. *Nanoscale* **2014**, *6*, 9734–9741.
- (80) Yin, H. J.; Zhao, S. L.; Wan, J. W.; Tang, H. J.; Chang, L.; He, L. C.; Zhao, H. J.; Gao, Y.; Tang, Z. Y. Three-Dimensional Graphene/
- Metal Oxide Nanoparticle Hybrids for High-Performance Capacitive Deionization of Saline Water. *Adv. Mater.* **2013**, *25*, 6270–6276.
- (81) Chen, W. F.; Li, S. R.; Chen, C. H.; Yan, L. F. Self-Assembly and Embedding of Nanoparticles by In Situ Reduced Graphene for Preparation of a 3D Graphene/Nanoparticle Aerogel. *Adv. Mater.* **2011**, *23*, 5679–5683.
- (82) Kim, F.; Cote, L. J.; Huang, J. X. Graphene Oxide: Surface Activity and Two-Dimensional Assembly. *Adv. Mater.* **2010**, *22*, 1954–1958.
- (83) Kim, J.; Cote, L. J.; Kim, F.; Yuan, W.; Shull, K. R.; Huang, J. X. Graphene Oxide Sheets at Interfaces. *J. Am. Chem. Soc.* **2010**, *132*, 8180–8186.
- (84) Li, Y. R.; Chen, J.; Huang, L.; Li, C.; Hong, J. D.; Shi, G. Q. Highly Compressible Macroporous Graphene Monoliths via an Improved Hydrothermal Process. *Adv. Mater.* **2014**, *26*, 4789–4793.
- (85) Barg, S.; Perez, F. M.; Ni, N.; Pereira, P. D. V.; Maher, R. C.; Garcia-Tunn, E.; Eslava, S.; Agnoli, S.; Mattevi, C.; Saiz, E. Mesoscale Assembly of Chemically Modified Graphene into Complex Cellular Networks. *Nat. Commun.* **2014**, *5*, 4328.
- (86) Chen, C. M.; Zhang, Q.; Huang, C. H.; Zhao, X. C.; Zhang, B. S.; Kong, Q. Q.; Wang, M. Z.; Yang, Y. G.; Cai, R.; Su, D. S. Macroporous ‘Bubble’ Graphene Film via Template-Directed Ordered-Assembly for High Rate Supercapacitors. *Chem. Commun.* **2012**, *48*, 7149–7151.
- (87) Zhang, Z. Y.; Xiao, F.; Xi, J. B.; Sun, T.; Xiao, S.; Wang, H. R.; Wang, S.; Liu, Y. Q. Encapsulating Pd Nanoparticles in Double-Shelled Graphene@Carbon Hollow Spheres for Excellent Chemical Catalytic Property. *Sci. Rep.* **2014**, *4*, 4053.
- (88) Zhang, R. J.; Cao, Y. C.; Li, P. X.; Zang, X. B.; Sun, P. Z.; Wang, K. L.; Zhong, M. L.; Wei, J. Q.; Wu, D. H.; Kang, F. Y.; et al. Three-Dimensional Porous Graphene Sponges Assembled with the Combination of Surfactant and Freeze-Drying. *Nano Res.* **2014**, *7*, 1477–1487.
- (89) Wang, X. B.; Zhang, Y. J.; Zhi, C. Y.; Wang, X.; Tang, D. M.; Xu, Y. B.; Weng, Q. H.; Jiang, X. F.; Mitome, M.; Golberg, D.; et al. Three-Dimensional Strutted Graphene Grown by Substrate-Free Sugar Blowing for High-Power-Density Supercapacitors. *Nat. Commun.* **2013**, *4*, 2905.
- (90) Zhao, Y.; Liu, J.; Hu, Y.; Cheng, H. H.; Hu, C. G.; Jiang, C. C.; Jiang, L.; Cao, A. Y.; Qu, L. T. Highly Compression-Tolerant Supercapacitor Based on Polypyrrole-Mediated Graphene Foam Electrodes. *Adv. Mater.* **2013**, *25*, 591–595.
- (91) Tao, Y.; Xie, X. Y.; Lv, W.; Tang, D. M.; Kong, D. B.; Huang, Z. H.; Nishihara, H.; Ishii, T.; Li, B. H.; Golberg, D.; et al. Towards Ultrahigh Volumetric Capacitance: Graphene Derived Highly Dense but Porous Carbons for Supercapacitors. *Sci. Rep.* **2013**, *3*, 2975.
- (92) Bi, H. C.; Yin, K. B.; Xie, X.; Zhou, Y. L.; Wan, N.; Xu, F.; Banhart, F.; Sun, L. T.; Ruoff, R. S. Low Temperature Casting of Graphene with High Compressive Strength. *Adv. Mater.* **2012**, *24*, 5124–5129.
- (93) Worsley, M. A.; Charnvanichborikarn, S.; Montalvo, E.; Shin, S. J.; Tylski, E. D.; Lewicki, J. P.; Nelson, A. J.; Satcher, J. H.; Bieker, J.; Baumann, T. F.; et al. Toward Macroscale, Isotropic Carbons with Graphene-Sheet-Like Electrical and Mechanical Properties. *Adv. Funct. Mater.* **2014**, *24*, 4259–4264.
- (94) Lv, W.; Xia, Z. X.; Wu, S. D.; Tao, Y.; Jin, F. M.; Li, B. H.; Du, H. D.; Zhu, Z. P.; Yang, Q. H.; Kang, F. Y. Conductive Graphene-Based Macroscopic Membrane Self-Assembled at a Liquid–Air Interface. *J. Mater. Chem.* **2011**, *21*, 3359–3364.
- (95) Shao, J. J.; Lv, W.; Guo, Q. G.; Zhang, C.; Xu, Q.; Yang, Q. H.; Kang, F. Y. Hybridization of Graphene Oxide and Carbon Nanotubes at the Liquid/Air Interface. *Chem. Commun.* **2012**, *48*, 3706–3708.
- (96) Lv, W.; You, C. H.; Wu, S. D.; Li, B. H.; Zhu, Z. P.; Wang, M. Z.; Yang, Q. H.; Kang, F. Y. pH-Mediated Fine-Tuning of Optical Properties of Graphene Oxide Membranes. *Carbon* **2012**, *50*, 3233–3239.
- (97) Lv, W.; Li, Z. J.; Zhou, G. M.; Shao, J. J.; Kong, D. B.; Zheng, X. Y.; Li, B. H.; Li, F.; Kang, F. Y.; Yang, Q. H. Tailoring Microstructure of Graphene-Based Membrane by Controlled Removal of Trapped

- Water Inspired by the Phase Diagram. *Adv. Funct. Mater.* **2014**, *24*, 3456–3463.
- (98) Shen, T.-Z.; Hong, S.-H.; Song, J.-K. Electro-Optical Switching of Graphene Oxide Liquid Crystals with an Extremely Large Kerr Coefficient. *Nat. Mater.* **2014**, *13*, 394–399.
- (99) Li, N.; Zhang, Q.; Gao, S.; Song, Q.; Huang, R.; Wang, L.; Liu, L. W.; Dai, J. W.; Tang, M. L.; Cheng, G. S. Three-Dimensional Graphene Foam as a Biocompatible and Conductive Scaffold for Neural Stem Cells. *Sci. Rep.* **2013**, *3*, 1604.
- (100) Yin, S.; Wu, Y.-L.; Hu, B.; Wang, Y.; Cai, P.; Tan, C. K.; Qi, D.; Zheng, L.; Leow, W. R.; Tan, N. S.; et al. Three-Dimensional Graphene Composite Macroscopic Structures for Capture of Cancer Cells. *Adv. Mater. Interfaces* **2014**, *1*, 1300043.
- (101) Zhao, J. P.; Ren, W. C.; Cheng, H. M. Graphene Sponge for Efficient and Repeatable Adsorption and Desorption of Water Contaminations. *J. Mater. Chem.* **2012**, *22*, 20197–20202.
- (102) Han, Z.; Tang, Z. H.; Shen, S. L.; Zhao, B.; Zheng, G. P.; Yang, J. H. Strengthening of Graphene Aerogels with Tunable Density and High Adsorption Capacity Towards Pb²⁺. *Sci. Rep.* **2014**, *4*, 5025.
- (103) Li, Z. J.; Lv, W.; Zhang, C.; Qin, J. W.; Wei, W.; Shao, J. J.; Wang, D. W.; Li, B. H.; Kang, F. Y.; Yang, Q. H. Nanospace-Confining Formation of Flattened Sn Sheets in Pre-Seeded Graphenes for Lithium Ion Batteries. *Nanoscale* **2014**, *6*, 9554–9558.
- (104) Qin, J.; Lv, W.; Li, Z.; Li, B.; Kang, F.; Yang, Q.-H. An Interlaced Silver Vanadium Oxide–Graphene Hybrid with High Structural Stability for Use in Lithium Ion Batteries. *Chem. Commun.* **2014**, *50*, 13447–13450.
- (105) Xie, T. T.; Lv, W.; Wei, W.; Li, Z. J.; Li, B. H.; Kang, F. Y.; Yang, Q. H. A Unique Carbon with a High Specific Surface Area Produced by the Carbonization of Agar in the Presence of Graphene. *Chem. Commun.* **2013**, *49*, 10427–10429.
- (106) Xie, X. Y.; Zhang, C.; Wu, M. B.; Tao, Y.; Lv, W.; Yang, Q. H. Porous MnO₂ for Use in a High Performance Supercapacitor: Replication of a 3d Graphene Network as a Reactive Template. *Chem. Commun.* **2013**, *49*, 11092–11094.
- (107) Liu, J. J.; Lv, W.; Wei, W.; Zhang, C.; Li, Z. J.; Li, B. H.; Kang, F. Y.; Yang, Q. H. A Three-Dimensional Graphene Skeleton as a Fast Electron and Ion Transport Network for Electrochemical Applications. *J. Mater. Chem. A* **2014**, *2*, 3031–3037.
- (108) Zhou, G. M.; Yin, L. C.; Wang, D. W.; Li, L.; Pei, S. F.; Gentle, I. R.; Li, F.; Cheng, H. M. Fibrous Hybrid of Graphene and Sulfur Nanocrystals for High-Performance Lithium-Sulfur Batteries. *ACS Nano* **2013**, *7*, 5367–5375.
- (109) Zhou, G. M.; Li, F.; Cheng, H. M. Progress in Flexible Lithium Batteries and Future Prospects. *Energy Environ. Sci.* **2014**, *7*, 1307–1338.
- (110) Wu, Z. S.; Yang, S. B.; Sun, Y.; Parvez, K.; Feng, X. L.; Mullen, K. 3D Nitrogen-Doped Graphene Aerogel-Supported Fe₃O₄ Nanoparticles as Efficient Electrocatalysts for the Oxygen Reduction Reaction. *J. Am. Chem. Soc.* **2012**, *134*, 9082–9085.
- (111) Xu, Y. X.; Lin, Z. Y.; Huang, X. Q.; Wang, Y.; Huang, Y.; Duan, X. F. Functionalized Graphene Hydrogel-Based High-Performance Supercapacitors. *Adv. Mater.* **2013**, *25*, 5779–5789.
- (112) Liu, T.; Kavian, R.; Kim, I.; Lee, S. W. Self-Assembled, Redox-Active Graphene Electrodes for High-Performance Energy Storage Devices. *J. Phys. Chem. Lett.* **2014**, *5*, 4324–4330.
- (113) Wu, Z. S.; Winter, A.; Chen, L.; Sun, Y.; Turchanin, A.; Feng, X. L.; Mullen, K. Three-Dimensional Nitrogen and Boron Co-Doped Graphene for High-Performance All-Solid-State Supercapacitors. *Adv. Mater.* **2012**, *24*, 5130–5135.
- (114) Yang, X. W.; Cheng, C.; Wang, Y. F.; Qiu, L.; Li, D. Liquid-Mediated Dense Integration of Graphene Materials for Compact Capacitive Energy Storage. *Science* **2013**, *341*, 534–537.
- (115) Zhang, C.; Liu, D.; Lv, W.; Wang, D.; Wei, W.; Zhou, G.; Wang, S.; Li, F.; Li, B.; Kang, F.; et al. A Highly Dense Graphene–Sulfur Assembly: A Promising Cathode for Compact Li–S Batteries. *Nanoscale* **2015**, DOI: 10.1039/C4NR06863G.